Journal of Hydrology 511 (2014) 811–824

Contents lists available at ScienceDirect

Journal of Hydrology

journal homepage: www.elsevier.com/locate/jhydrol

Temporal and spatial variations in radiation and energy balance across a large freshwater lake in China

Wei Wang [a], Wei Xiao [a], Chang Cao [a], Zhiqiu Gao [a,b], Zhenghua Hu [a], Shoudong Liu [a], Shuanghe Shen [c], Linlin Wang [b], Qitao Xiao [a], Jiaping Xu [a], Dong Yang [a], Xuhui Lee [a,d,*]

[a] Yale-NUIST Center on Atmospheric Environment, Nanjing University of Information Science and Technology, Nanjing 210044, China
[b] State Key Laboratory of Atmospheric Boundary Layer Physics and Atmospheric Chemistry, Institute of Atmospheric Physics, Chinese Academy of Sciences, Beijing 100029, China
[c] Jiangsu Key Laboratory of Agricultural Meteorology, Nanjing University of Information Science and Technology, Nanjing 210044, China
[d] School of Forestry and Environmental Studies, Yale University, New Haven, CT 06511, USA

ARTICLE INFO

Article history:
Received 8 August 2013
Received in revised form 12 January 2014
Accepted 2 February 2014
Available online 15 February 2014
This manuscript was handled by Konstantine P. Georgakakos, Editor-in-Chief, with the assistance of Ana P. Barros, Associate Editor

Keywords:
Eddy covariance
Lake Taihu
Energy balance
Evaporation
Bowen ratio

ABSTRACT

The surface radiation and energy exchange processes are important drivers of lake evaporation and the associated hydrological cycle. In this paper, we investigated the temporal and spatial variations in evaporation and the associated radiation and energy fluxes across Lake Taihu, China with an eddy covariance mesonet consisting of three lake sites and one land site. The results indicate that on the diurnal scale, water heat storage showed a similar behavior to net radiation with comparable magnitudes and fueled the substantial nighttime evaporation (48% of annual evaporation). Unlike boreal deep lakes, the monthly mean sensible and latent heat flux was tightly coupled with seasonal variations in net radiation at this large (size 2400 km^2), subtropical (30.9–31.6°N) shallow (mean depth 1.9 m) Lake Taihu. On the monthly to annual scales, the radiation and energy fluxes showed little spatial variations across the lake, indicating a lack of sensitivity to wind speed, water depth, water quality and the presence of submerged macrophytes. The annual mean Bowen ratio (0.12–0.13) of the lake was lower than those found in the literature for subtropical and northern lakes and also much lower than that observed at the adjacent land site (0.58). The experimental data were used to evaluate the performance of 19 lake evaporation models of varying complexities.

1. Introduction

This study is concerned with the radiation, energy and water vapor fluxes of Lake Taihu, a large (size 2400 km^2) and shallow (mean depth 1.9 m) freshwater lake in southern China. The surface radiation and energy exchange processes are important drivers of lake evaporation and the associated hydrological cycle (Stephens et al., 2012; Verburg and Antenucci, 2010). Our experimental data were obtained with an eddy covariance (EC) network consisting of three sites in the lake and one site on land. Since the 1990s, the EC technique has been widely used to measure heat, water vapor and momentum fluxes in numerous upland ecosystems (e.g., Aubinet et al., 2000; Baldocchi et al., 2001). Although logistically difficult, in recent years the technique has also been used in an increasing number of long-term field campaigns on lake-air interaction (Blanken et al., 2003, 2011; Liu et al., 2012a; Nordbo et al., 2011; Rouse et al., 2008). EC provides a more accurate alternative to the water balance method in the determination of lake evaporation because the water balance method can suffer from large uncertainties (especially for large lakes) due to the difficulty in measuring the inflows and outflows and in measuring precipitation over the lake. To date, most of the published EC observations were conducted in deep boreal lakes. Year-round EC observations in shallow lakes in more southern latitudes are still rare (Liu et al., 2012a).

Currently our knowledge is relatively poor on processes that drive shallow lake evaporation in subtropical climates. Subtropical shallow lakes differ from northern deep lakes in several respects. First, deep boreal or temperate lakes are usually dimictic: they experience turnover in the spring and the autumn, and are thermally stratified in the summer (Oswald and Rouse, 2004). In comparison, shallow lakes experience turnover occurrence at the diurnal scale, with the static stability oscillating between stable stratification in the daytime and convective unstable conditions during the nighttime (Deng et al., 2013). Second, the time lag between water and air temperature can be as long as 5 months

* Corresponding author at: School of Forestry and Environmental Studies, Yale University, Kroon Hall, 195 Prospect Street, New Haven, CT 06511, USA. Tel.: +1 (203)432 6271; fax: +1 (203)432 5023.
E-mail address: xuhui.lee@yale.edu (X. Lee).

http://dx.doi.org/10.1016/j.jhydrol.2014.02.012
0022-1694/

for deep lakes (Blanken et al., 2011) but negligible for shallow lakes (Deng et al., 2013; Oswald and Rouse, 2004). Third, southern lakes are ice-free, whereas ice coverage occurs in northern lakes, effectively decoupling the lake-atmosphere interactions in the winter. It is shown that in northern latitudes, global circulation patterns such as ENSO can modulate ice duration and phenology, two important factors controlling the annual lake evaporation (Bai and Wang, 2012; Blanken et al., 2000, 2011). Such linkages are absent for ice-free lakes. In these regards, subtropical shallow lakes should evaporate more water vapor and respond more quickly to atmospheric forcings than northern deep lakes at the diurnal and seasonal scales.

Several considerations support the hypothesis that across immense lakes like Lake Taihu, lake evaporation should vary spatially due to spatial heterogeneity in biophysical properties of the lake. Variations in water pollution (Wang et al., 2011) are likely to generate variations in the turbulent fluxes due to the attenuation of solar radiation by the pollutants (Huang et al., 2009). Having lower heat capacity, shallow parts of the lake may undergo faster warming and cooling than the deep parts, resulting in spatial variability of water temperature. For instance, the near-shore surface temperature was 10 °C warmer than at the deepest region in the Great Slave Lake, in Canada after ice breakup (Schertzer et al., 2003). Wind speed, which is a meteorological variable regulating the turbulent fluxes, tends to be stronger, because of the open fetch, in the middle of the lake than in the near-shore environment (Schertzer et al., 2003). In addition, the heat, water vapor and momentum transfer coefficients are known to vary with wind speed and submerged vegetation (Xiao et al., 2013). Largely because of these spatial heterogeneities, errors in the daily lake evaporation estimate may be as large as 100% if the whole-lake evaporation is evaluated on observations made at a single location (Assouline and Mahrer, 1996). Furthermore, spatial variability of evaporation at Lake Superior can be as large as 7 mm d^{-1} in the winter (Spence et al., 2011). So far, the discussion on these spatial variability has been based on the bulk transfer relationships for the fluxes aided by meteorological variables from numerical weather predictions (Spence et al., 2011) or remote sensing and buoy observations (Laird and Kristovich, 2002; Lofgren and Zhu, 2000). Our work appears to represent the first attempt at testing the hypothesis on the evaporation spatial variability on the seasonal and annual time scales using direct flux observations.

The energy and water fluxes of a lake differ from those in the surrounding vegetated terrain because of its low surface albedo, large heat capacity, unlimited water supply and low surface roughness (Henderson-Sellers, 1986; Subin et al., 2012; Venäläinen et al., 1999). Quantifying these contrasts is a critical step for accurate prediction of local thermal circulations (Crosman and Horel, 2010, 2012; Steyn, 2003) and the associated dispersion and transport of air pollutants (Flagg et al., 2008; Sills et al., 2011). There are five cities with population greater than 1 million around Lake Taihu, so it is important to understand how pollution dispersion is impacted by lake–land circulations and boundary layer dynamics. So far there have been few concurrent EC observations that compare lake energy and water fluxes with those on the adjacent land (Claussen, 1991; Eaton et al., 2001; Oncley et al., 1997; Venäläinen et al., 1999).

From the modeling perspective, there exist a large number of lake evaporation models of varying complexities (Brutsaert, 1982; Elsawwaf et al., 2010a; Rosenberry et al., 2007; Winter et al., 1995). So far, few studies have compared these models against a common EC dataset to evaluate their performance (Tanny et al., 2008, 2011). In this regard, the availability of the data on the lake surface radiation and energy balance is crucial because the most accurate lake evaporation models are believed to be those that have incorporated the radiation and energy balance constraints, such as the Bowen ratio energy budget model and the Priestley–Taylor model (Elsawwaf et al., 2010a, 2010b; Rosenberry et al., 2007; Winter et al., 1995).

In this paper, we aim to elucidate mechanisms underlying the observed temporal and spatial variations in radiation and energy fluxes across Lake Taihu. The goal is four-fold: (1) to quantify the evaporation and energy regimes through the diurnal and the seasonal cycle, (2) to test the hypothesis that there should exist discernible spatial variations in the energy and water fluxes across the lake, (3) to compare and contrast the fluxes between the lake and the surrounding land surface, and (4) to evaluate the accuracy of 19 classic evaporation models (Supplementary Table 1) against the EC observations.

2. Theoretical considerations

2.1. Surface energy balance

The energy balance of a lake surface is given by (Henderson-Sellers, 1986)

$$R_n - \Delta Q = H + \lambda E + \Delta Q_B + \Delta Q_F + \Delta Q_P \quad (1)$$

where R_n is net radiation, ΔQ is lake heat storage determined with the time rate of change of the depth-weighted mean water temperature, ΔQ_B is the heat flux into the sediment, ΔQ_F is the net heat flux carried by the inflow and outflow of the lake, and ΔQ_P is the heat flux resulted from precipitation. The last three terms are negligible for the following reasons. We did not measure ΔQ_B. According to Wang and Bras (1999), it can be estimated with the time series of the observed sediment temperature. Using the thermal conductivity for saturated soils, their model yielded ΔQ_B values less than 0.5 W m^{-2} in magnitude. Similarly, ΔQ_F was no more than 0.5 W m^{-2} with the inflow of 9.3×10^9 m^3 yr^{-1} and assuming a temperature difference of 1 °C between the inflows and the lake water (Qin et al., 2007). At the annual precipitation rate of 1100 mm, ΔQ_P was estimated to be −0.5 W m^{-2} on the assumption that the rainwater had the wet bulb temperature (Gosnell et al., 1995; Shoemaker et al., 2005). Thus omitting the minor terms, the surface energy balance equation is reduced to:

$$R_n - \Delta Q = H + \lambda E \quad (2)$$

Similarly, the energy balance equation of the land surface is given by

$$R_n - G = H + \lambda E \quad (3)$$

where G is the heat flux at the soil surface.

For the lake sites, the energy balance closure can be assessed by the ratio (EBC, %) of the turbulent fluxes ($H + \lambda E$) to the available energy ($R_n - \Delta Q$):

$$\mathrm{EBC} = \frac{H + \lambda E}{R_n - \Delta Q} \times 100\% \quad (4)$$

or in terms of an absolute residual (Res, W m^{-2}):

$$\mathrm{Res} = R_n - \Delta Q - \lambda E - H \quad (5)$$

Eqs. (4) and (5) can be modified for the land site by simply replacing ΔQ with G.

2.2. Energy storage in the water column

The heat storage change (ΔQ) is determined by the variation in depth-weighted mean temperature ($d\overline{T_w}$) of the water column over the time interval (dt) (Blanken et al., 2000):

$$\Delta Q = \rho_w c_{pw} \int_0^z \frac{d\overline{T_w}}{dt} dz \quad (6)$$

where z is the depth of whole water column, ρ_w is water density, c_{pw} is specific heat of water. In practice, profile measurement of water temperature is conducted by a finite number of temperature probes in the vertical, and the variation in the depth-weighted mean temperature over a specified time interval (e.g., 30 min) can be calculated in the summation form:

$$\Delta\overline{T_w} = \frac{1}{z}\sum_{i=1}^{n}\Delta T_{w,i}\Delta z_i \quad (7)$$

where n (= 5) is the number of probes, $T_{w,i}$ is the water temperature at depth i, and Δz_i is the depth segment represented by $T_{w,i}$. Water depth at each site was updated daily based on water level observations.

2.3. Forcing energy balance closure

The problem of energy imbalance, that the sum of the turbulent fluxes is not equal to the available energy, is a long-standing issue for the micrometeorological community (Foken, 2008; Leuning et al., 2012; Wang and Dickinson, 2012). To produce robust spatial comparisons and obtain accurate lake evaporation, we adjusted the measured H and λE to force energy balance closure using the method of Twine et al. (2000). This method assumes that even though the EC turbulent fluxes (H and λE) are not measured accurately, the resulting Bowen ratio is accurate (Barr et al., 1994; Blanken et al., 1997). Then turbulent fluxes are adjusted without changing the Bowen ratio:

$$\beta = \frac{H}{\lambda E} \quad (8)$$

$$\lambda E^* = \frac{R_n - \Delta Q}{1+\beta} \quad (9)$$

$$H^* = R_n - \Delta Q - \lambda E^* \quad (10)$$

where β is the Bowen ratio, λE^* and H^* are the latent heat and sensible heat fluxes after forcing energy balance closure, respectively. These adjustments were done to the monthly mean fluxes but not to the 30-min fluxes (Wohlfahrt et al., 2009). At the 30-min interval, attributing the residual energy to H and λE by preserving Bowen ratio can result in an abnormally negative ($<-100\ W\ m^{-2}$) λE^*, especially at the DS site during the nighttime; these negative values are much too large in comparison to fluxes during dew events and are physically unreasonable.

2.4. Lake evaporation models

The 19 evaporation models selected for evaluation were grouped into five methodological categories according to the underlying theoretical constraints and the data requirements: (1) the combination group, (2) the solar radiation–temperature group, (3) the Dalton group, (4) the temperature–daylength group, and (5) the temperature group (Supplementary Table 1). The combination group, based on the principles of energy balance closure and the flux-gradient theory, is the most comprehensive in explaining the evaporation process, but is also the most data-intensive (Elsawwaf et al., 2010a; Rosenberry et al., 2007). The radiation–temperature models estimate evaporation simply by the product of a global radiation and an air temperature function with empirical coefficients developed for specific climates (McMahon et al., 2013; Tabari, 2010). Similarly, the temperature–daylength models predict evaporation empirically by deploying functions of daylight duration and air temperature. In the Dalton models, the evaporation rate is proportional to the specific humidity difference between the lake surface and a reference height, with the proportionality being the Dalton number. Models belonging to the temperature group, such as the Papadakis and Thornthwaite models, are least data demanding but have rarely been applied to estimate lake evaporation (Elsawwaf et al., 2010a).

3. Experimental method

3.1. Sites

Lake Taihu is the third largest freshwater lake in China, with a surface area of 2400 km^2 and a mean depth of 1.9 m. It receives an annual inflow of $9.3 \times 10^9\ m^3$. The lake surface elevation is 3 m above the mean sea level. The lake catchment is 37,000 km^2 in size. The experiment was conducted at the Lake Taihu eddy covariance mesonet consisting of Meiliangwan (MLW), Dapukou (DPK) and Bifenggang (BFG), situated in the north, west and east part of the lake (Fig. 1). A companion land site was located in the Dongshan (DS) Peninsula on the southeast shore of the lake. The linear distance to the nearest shoreline is 150 m for MLW, 2.0 km for DPK, 4 km for BFG and 1.5 km for DS. The EC and meteorological observations commenced on June 14, 2010 at MLW, August 18, 2011 at DPK (December 4, 2010 for radiation observations), December 15, 2011 at BFG and April 16, 2011 at DS. The data used in this study covered the periods from the commencement dates to August 31, 2012.

The three lake sites were characterized by different biophysical environments. DPK was the deepest (2.6 m) among the lake sites, and was windy, with a mean wind speed of 3.7 m s^{-1} at the height of 2 m above the surface from September 2011 to August 2012. The wind direction from the open water (345–360 deg and 0–245 deg) comprised ~85% of the observations; in these wind direction ranges the upwind fetch was greater than 3 km, guaranteeing that its measurements were representative of the open water of this immense lake. DPK was subject to frequent algal blooms in the spring and summer and was constantly turbid because of wind-induced suspended sediment (Wang et al., 2011). High level of dissolved organic carbon was often observed due to pollutant inputs by river inflows (Zhang et al., 2011; Fig. 1).

The most outstanding feature of BFG is that the aquatic ecosystem was dominated by submerged macrophytes (mainly *Potamogeton malaianus* and *Hydrilla verticillata*). The presence of these macrophytes reduces the momentum flux by ~40% (Xiao et al., 2013) through the suppression of wind-induced waves and therefore surface roughness (Madsen et al., 2001), but its effects on evaporation, sensible heat and radiation flux are not known. The fetch at BFG was greater than 4 km in all wind directions. The site was also windy: the 2-m wind speed was 4.0 m s^{-1} from January 2012 to August 2012. At BFG, the water was much cleaner than at DPK and MLW (Liu et al., 2013).

Because of its proximity to the shoreline, the turbulent fluxes at MLW were contaminated by the surrounding land when wind direction fell in the ranges of 0–200 deg and 315–360 deg, which occurred ~83% of the time. This site had a weaker wind speed than the other two lake sites: the 2-m wind speed was 2.4 m s^{-1} from September 2011 to August 2012. Like DPK, MLW was subject to frequent algal blooms in the spring and summer, and high chlorophyll-a (Wang et al., 2011) and dissolved organic carbon concentration all year round (Zhang et al., 2011).

DS was a land site in a landscape dominated by cropland and rural houses. It had a similar wind speed (2.3 m s^{-1}) to MLW at the 2-m height above the surface.

3.2. Instrumentation

At every site, there were an EC system, a 4-component net radiometer, a standard micrometeorological system and sensors for

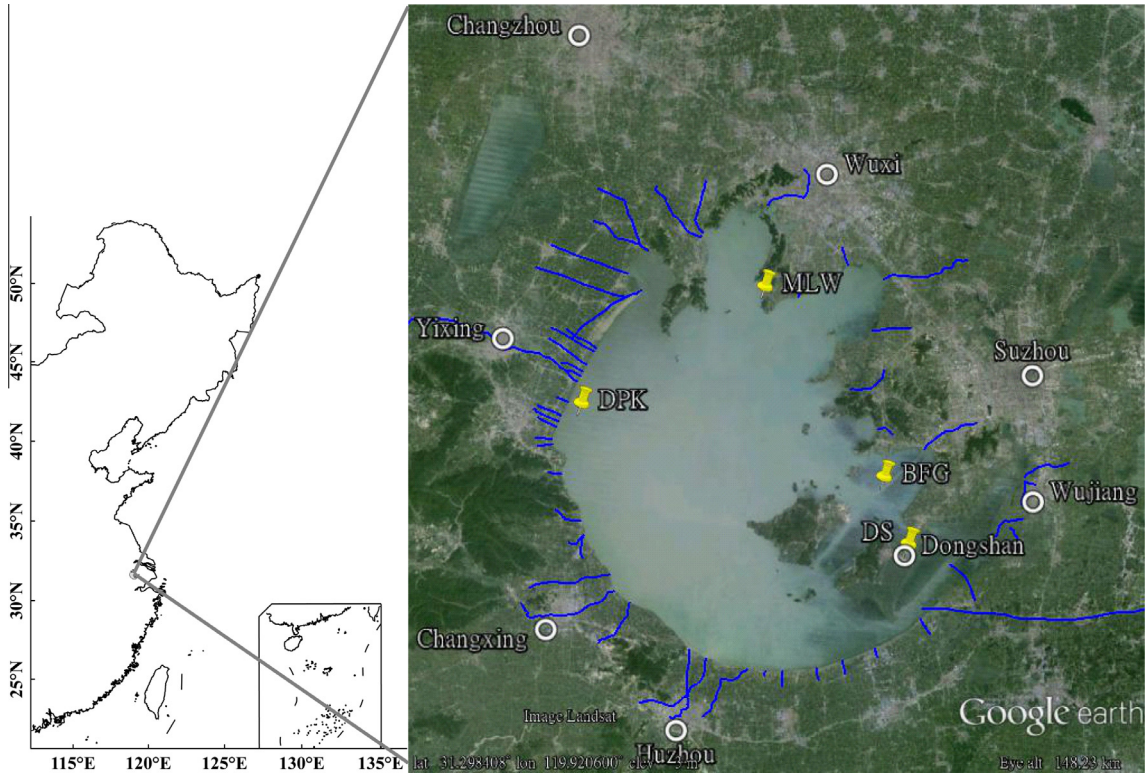

Fig. 1. Map showing the eddy covariance mesonet at Lake Taihu consisting of three lake sites (Meiliangwan, MLW; Dapukou, DPK; Bifenggang, BFG) and one land site (Dongshan, DS) (yellow pins). Six standard weather stations (white circles) near the lake and 51 main inflows/outflows (blue lines) of Lake Taihu are also indicated. (For interpretation of the references to color in this figure legend, the reader is referred to the web version of this article.)

measuring water or soil temperature profile. The instruments were mounted on rigid platforms at DPK and BFG, on a concrete pillar at MLW in the lake, and on a 30-m tall tower at DS.

The EC system, consisting of a three-dimensional sonic anemometer/thermometer (model CSAT3, Campbell Scientific Inc., Logan, UT, USA) and an open-path infrared gas analyzer (model EC150, Campbell Scientific Inc. at BFG; model LI7500A, Li-Cor Inc., Lincoln, NE, USA at the other three sites), was employed to measure the three dimensional wind speeds and atmospheric H_2O and CO_2 concentration at 10 Hz. Fluxes of momentum (τ), sensible heat (H) and latent heat (λE) were calculated from the 10 Hz time series over 30-min intervals and were recorded by a datalogger (model CR3000, Campbell Scientific Inc.). Coordinate rotation was performed according to the natural wind coordinate system (Lee et al., 2004). Density corrections were applied to λE and the CO_2 flux (Lee and Massman, 2011; Webb et al., 1980). The EC measurement height was 8.5 m at DPK, 3.5 m at MLW, 8.5 m at BFG and 20 m at DS.

A suite of auxiliary variables were observed as 30-min means. A net radiometer (model CNR4, Kipp & Zonen B.V., Delft, The Netherlands) was used to measure the incoming shortwave ($K_\downarrow$), reflected shortwave ($K_\uparrow$), incoming longwave ($L_\downarrow$) and outgoing longwave radiation ($L_\uparrow$). A micrometeorology system (model Dynamet, Dynamax Inc., Houston, TX, USA) was used to measure air temperature (T_a), relative humidity (RH), wind speed (U) and wind direction. Additionally, at the DS site, gradient measurements of T_a, RH and wind were conducted at the height of 10, 20, 25 m above the land surface with temperature/humidity probes (model HMP155A, Vaisala Inc., Helsinki, Finland) and wind speed sensors (model 05103, R.M. Young Company, Traverse City, MI, USA). Precipitation was measured by an automated tipping-bucket rain gauge (model TE525-L, Campbell Scientific Inc.). Temperature probes (model 109-L, Campbell Scientific Inc.) were placed at the 20, 50, 100 and 150 cm depth and in the surface sediment to measure the water (T_w) and sediment temperature at the lake sites. At the DS land site, soil temperature at the 5, 10, 15 cm depth was measured with the probes of the same type. The skin temperature (T_s) was solved from the outgoing longwave radiation using the Stefan–Boltzmann law with an emissivity of 0.97 for water and 0.93 for the land surface (Arya, 2001; Fiebrich et al., 2003).

The water temperature profile data were used to determine the heat storage in the water column (Eqs. (6) and (7)). The accuracy of the temperature sensors was ±0.25 °C over the range of −10 °C to 70 °C in the worst case (Campbell Scientific, 2011). To minimize systematic bias errors, the probes were inter-compared once a month by placing all of them at the same depth (20 cm) for 2–6 h; any relative differences were removed prior to the heat storage calculation. Furthermore, a three-point (1.5 h) running mean was applied to lower the random error of the water temperature data.

3.3. Data gaps

In order to produce monthly mean values, we filled the missing data in the following manners. The gap fraction in the radiation measurements was less than 6% at the lake sites; these gaps were filled by the observations available from the other sites. In the case of H and λE, the data were kept for further calculation of the daily mean if the 30-min flux data were available for more than 85% of a day and were discarded otherwise. Using this criterion, the gap fraction was 37%, 37%, 35% and 36% at MLW, DPK, BFG and DS sites respectively. Missing daily mean H and λE were gap-filled using the bulk transfer relationship (Garratt, 1992; Laird and Kristovich, 2002; Liu et al., 1979) with the transfer coefficient determined with the valid daily data. More specifically, gaps in H were filled with a function described by the product of wind speed and temperature difference between the surface and overlaying atmosphere (Fig. 2a and c). Gaps in λE were filled with a function describing the dependence on wind speed and vapor pressure

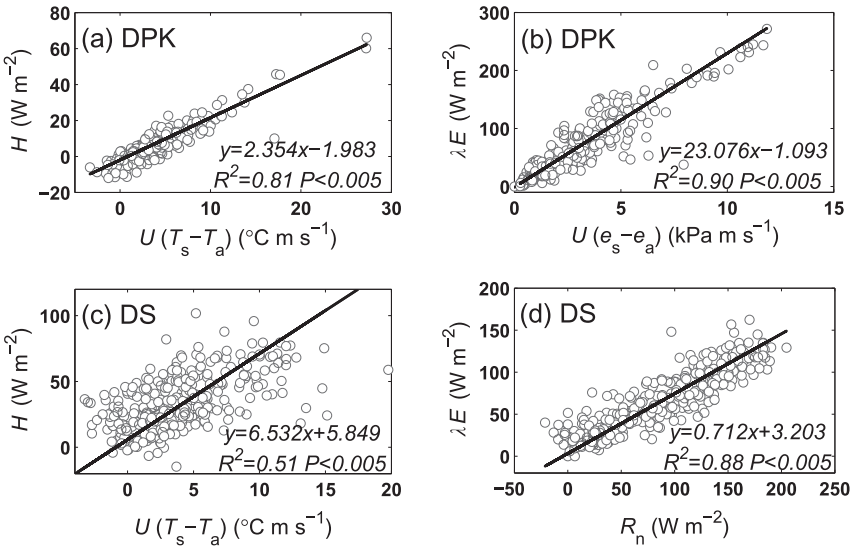

Fig. 2. Scatter plot showing the bulk transfer relationship for the daily mean sensible (H) and latent heat flux (λE) for DPK and DS. Here, U is wind speed, T_a is air temperature, T_s is surface temperature, e_a is atmospheric vapor pressure, e_s is the saturation vapor pressure at the surface temperature, and R_n is net radiation. Lines represent geometric mean regression with regression statistics noted. Similar bulk relationships were also found for MLW and BFG.

difference between the surface and overlying atmosphere for the lake sites (Fig. 2b) and a function relating the flux to net radiation for the land site (Fig. 2d). These bulk transfer relationships for gap filling were justified because they have a mechanistic foundation and explained a high percentage of the observed variations in the fluxes (R^2 > 50% for H and R^2 > 88% for λE).

4. Results and discussion

4.1. Energy balance closure

The monthly EBC averaged over the observation period was 69% at MLW, 75% at DPK, 71% at BFG and 111% at DS. The residual shows a clear seasonal pattern being larger in the months with higher R_n, with the annual average values of 28.3, 22.5 and −8.5 W m^{-2} at MLW, DPK and DS, respectively, and 24.4 W m^{-2} at BFG over the observation period. Our EBC values are comparable to those reported (around 80%) from EC observations on land (Beer et al., 2010; Foken, 2008; Twine et al., 2000; Wilson et al., 2002b) and a few EC campaigns over lakes (Table 1). Wilson et al. (2002b) suggest that energy imbalance for smooth surfaces such as lakes should be worse than that for rough terrestrial ecosystems such as forests. Contributors to energy imbalance of dry-land ecosystems include incapable detection of low-frequency and high-frequency eddies and mismatch in source areas of the eddy fluxes and fluxes of net radiation and heat storage (Foken, 2008; Leuning

Table 1
A summary of the energy balance closure from eddy covariance measurement in lakes.

Lake name	Location	Area (km^2)	Mean depth (m)	Maximum depth (m)	Observation period	EBC (%)	Residual (W m^{-2})	Reference
Lake Taihu, China	31°25′N, 120°13′E (MLW)	2,400	1.9	2.5	July, 2010–August, 2012	69	28	This study
	31°15′N, 119°55′E (DPK)		2.6	3.1	September, 2011–August, 2012	75	22	
	31°10′N, 120°24′E (BFG)		1.8	2.4	January, 2012–August, 2012	71	24	
Ross Barnett Reservoir, USA	32°26′N, 90°02′W	130	5	8	January–December, 2008	97	3	Liu et al. (2012a)
Erhai Lake, China	25°45′N, 100°11′E	250	11	21.5	January–December, 2011	80 (summer), 70 (other time)		Liu et al. (2012b)
Lake Valkea-Kotinen, Finland	61°14′N, 25°03′E	0.041	2.5	6.5	Open water period 2005–2008	82 (2006), 73 (2007)	16 (2006), 22 (2007)	Nordbo et al. (2011)
Lake Merasjärvi, Sweden	67°33′N, 21°58′E	3.8	5.1	17	July 29–August 2, 2005	80	20	Jonsson et al. (2008)
Eshkol Reservoir, Isreal	32°46′N, 35°15′E	0.36	3.5		September 2–10, 13–17, 2005	92	15	Tanny et al. (2008)
					May–August, 2008	70		Tanny et al. (2011)
Lake Tämnaren, Sweden	60°00′N, 17°20′E	37	1.2	2	Week 19–25, 1995	53	53	Elo (2007)
Lake Råksjö, Sweden	60°02′N, 17°05′E	1.5	4.3	10.5	Week 21–34, 1995	63	42	Elo (2007)
Lake Soppensee, Switzerland	47°05′N, 8°05′E	0.25	12	27	September 21–23, 1998		<10	Eugster et al. (2003)
Great Slave Lake, Canada	61°55′N, 113°44′W	27,000	41	614	July 24–September 10, 1997	96		Blanken et al. (2000)

et al., 2012). For lake sites, intensive turbulence can cause fluctuations in water temperature profile measurements, which may introduce noises to the estimation of ΔQ (Nordbo et al., 2011). Energy imbalance may also be exacerbated by horizontal heat transport via water currents (Jonsson et al., 2008), which are on the order of 10–30 cm s^{-1} at Lake Taihu (Qin et al., 2000). Furthermore, advection fluxes associated with the large roughness and thermal contrasts between the water surface and the adjacent land may also contribute to low EBC (Vesala et al., 2006).

After adjustment for energy balance (Section 2.3), the annual mean H was enhanced by 3.3, 2.7 and 2.1 W m^{-2}, and λE by 25, 19.7 and 22.3 W m^{-2} at MLW, DPK and BFG, respectively. At the DS land site, H was reduced by 4.4 W m^{-2} and λE reduced by 4.1 W m^{-2}. In the following analysis, the monthly and annual flux values were based on the adjusted fluxes data.

4.2. Seasonal variations in the lake energy fluxes

Because of its long data record, MLW site is chosen here to depict the seasonal variations in the energy fluxes over Lake Taihu. Net radiation R_n and latent heat flux λE showed a strong seasonal cycle (Fig. 3e and f), but sensible heat flux H and heat storage ΔQ did not (Fig. 3d and g). Net radiation peaked in July or August and reached its minimum near the winter solstice (Fig. 3f), with monthly mean values ranging from the minimum of 27.6 W m^{-2} (December 2011) to the maximum of 176.3 W m^{-2} (July 2012). During the summer season, R_n showed some interannual variability due to variations in cloud cover: the July value was 139.9 W m^{-2} in 2010, 143.7 W m^{-2} in 2011 and 176.3 W m^{-2} in 2012. The wintertime value seemed to have a lower interannual variability, with the monthly mean of 27.9 W m^{-2} and 27.6 W m^{-2} for December 2011 and December 2012, respectively.

The seasonal course in λE (Fig. 3e) can be divided into a warming phase (January to July) and a cooling phase (August to December) according to the trend of the lake water and air temperature (Fig. 3a and b). During the warming phase, R_n was the main energy input to the lake system, and nearly 75% of it was used by evaporative loss, with the rest used to heat the atmosphere via H and to warm the lake water. The maximum monthly mean λE was 155.6 W m^{-2} (July 2012). In this phase, λE closely followed the temporal pattern of R_n. The maximum ratio of $\lambda E/R_n$ (90%) was observed in May 2011. In the cooling phase, λE reached its minimum (20.9 W m^{-2}) in January 2011, about one month later than the minimum of R_n. Similarly, latent heat flux also lags by one month behind net radiation at Sparkling Lake in northern Wisconsin, USA (mean depth 10.9 m; Lenters et al., 2005) and Lake

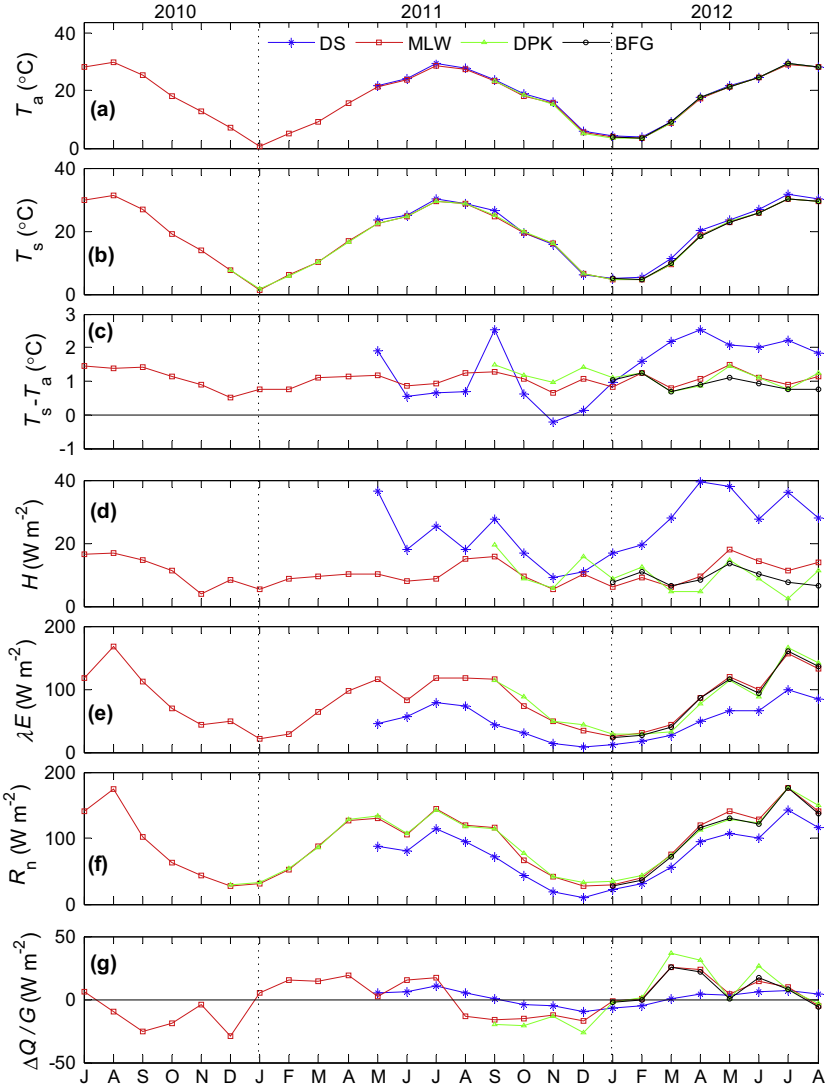

Fig. 3. Monthly mean (a) air temperature (T_a), (b) surface temperature (T_s), (c) difference between surface temperature and air temperature (T_s–T_a), (d) sensible heat flux (H), (e) latent heat flux (λE), (f) net radiation (R_n), (g) heat storage in water (ΔQ) or soil surface heat flux (G) at three lake sites (MLW, DPK and BFG) and one land site (DS).

Vegoritis, in Greece (mean depth 20 m; Gianniou and Antonopoulos, 2007). The phase lag is greater for deeper lakes with higher heat capacity. For example, Lake Ikeda, in Japan (mean depth 125 m) has a delay of 2 months (Momii and Ito, 2008) and phase lag of 5 months were found for Lake Superior, in North America (mean depth 148 m; Blanken et al., 2011).

The seasonal evolution of heat storage ΔQ consisted of a 7-month storage (January to July, $\Delta Q > 0$) and a 5-month release (August to December, $\Delta Q < 0$) (Fig. 3g). Compared to deep lakes, Lake Taihu has smaller thermal inertia owing to its shallow depth. Heat storage ranged from $-29.0\ W\ m^{-2}$ in December 2010 to $25.4\ W\ m^{-2}$ in March 2012, which is comparable in magnitude to that reported for an agricultural water reservoir in southern Spain (mean depth 5 m; Gallego-Elvira et al., 2010) and slightly smaller than the results at the Ross Barnett Reservoir in Mississippi, USA (depth 5 m; Liu et al., 2012a), but is one order of magnitude lower than that for Lake Superior (Blanken et al., 2011). In the winter months when R_n was low, the energy used for evaporation was partially drawn from the internal heat storage in Lake Taihu.

In comparison to the latent heat flux λE, sensible heat flux H was relatively small, with month mean values being less than $20\ W\ m^{-2}$. On the monthly basis, the lake surface temperature T_s of Lake Taihu was always higher than air temperature T_a (Fig. 3a–c), although inverse gradients happened occasionally on nights with low wind speed and clear skies. The water temperature at the 20 cm depth was 2.7, 0.6, and 1.2 °C higher than air temperature in August 2011, January 2012 and on the annual basis, respectively (Fig. 3a–c, Table 2). The much larger temperature gradient existed in August than in January because of stronger solar energy input in the summer than in the winter.

Bowen ratio (β) as an indicator of energy partitioning was quite small compared to that for land ecosystems (e.g., Eaton et al., 2001; Wilson et al., 2002a), increasing from 0.07 in July to 0.3 in February. Seasonality of β has been reported for temperate lakes. It increases from 0.1 in May to 0.85 in early November in Sparkling Lake (Lenters et al., 2005). Similar seasonality has also been found in Williams Lake, in the USA (Sturrock et al., 1992). For Lake Ikeda in similar climatic conditions to Lake Taihu, a gradual increase of β from −0.1 in April to 0.4 in the winter has been documented (Momii and Ito, 2008). There was no ice formation in Lake Taihu throughout the year, and its monthly mean β was always positive. In contrast, in deep temperate and boreal lakes, T_s can be lower than T_a in the late spring and early summer, causing negative β (Blanken et al., 2011; Momii and Ito, 2008).

4.3. Diurnal variations in the lake energy fluxes

The diurnal composite energy fluxes are presented for DPK, MLW and DS in Fig. 4. Computed as the average values of the valid half-hourly observations made at the same time of the day in a complete year (September 2011–August 2012), these composites have removed the influences of weather fluctuations and brought out clearly the diurnal variations. The reader is reminded that no energy balance adjustment was made to the 30-min observations. Dominated by the incoming shortwave radiation $K_\downarrow$, the composite R_n followed a smooth curve, peaking at solar noon and becoming negative during the nighttime (Fig. 4a–c). The 30-min R_n value ranged from $431.5\ W\ m^{-2}$ at 12:30 Beijing time to $-39.3\ W\ m^{-2}$ at midnight at DPK (Fig. 4a). The nighttime radiative cooling was attributed to a much stronger outgoing longwave radiation $L_\uparrow$ from the water body than the corresponding one from atmosphere ($L_\downarrow$).

The heat storage term ΔQ showed a similar diurnal behavior to R_n with comparable magnitudes (Fig. 4d and e). It peaked around noon with the value of $363.2\ W\ m^{-2}$ and reached its minimum at 19:30 with a value of $-166.1\ W\ m^{-2}$ at DPK (Fig. 4d). The heat release from the lake water during the nighttime ($\Delta Q < 0$) was strong enough to compensate the negative R_n, supplying energy to support the positive H and λE into the atmosphere.

Direct measurement of lake heat storage has been seldom reported for lack of measurement of the water temperature profile with high temporal resolutions. Instead it is often evaluated as the residual of the energy balance equation ($\Delta Q = R_n - H - \lambda E$) (Blanken et al., 2011; Venäläinen et al., 1999). A diurnal range between −100 and $400\ W\ m^{-2}$ was reported by Venäläinen et al. (1999) for Lake Råksjön, in Sweden from May to August 1995, and a smaller variation range from −210 to $280\ W\ m^{-2}$ was observed at Lake Valkea-Kotinen, in Finland in June 2007 (Nordbo et al., 2011).

The sensible heat flux H showed a much smaller diurnal variation than net radiation and heat storage. At DPK, the composite H varied from $0.1\ W\ m^{-2}$ at 18:00 to $13.3\ W\ m^{-2}$ at 9:30. This diurnal pattern follows closely to the temperature gradient between the lake surface (T_s) and the overlaying atmosphere (T_a), with the phase of the former lagging slightly behind that of the latter due to the water thermal inertia. Quantitatively, the temperature difference $T_s - T_a$ reached 1.7 °C around 9:30 and decreased to 0.3 °C around sunset. Similarly small diurnal variations of H were found in the shallow Swedish Lake Tämnaren (depth 1.2 m, 0 to $20\ W\ m^{-2}$; Venäläinen et al., 1999), whereas larger variations were observed in another Swedish Lake Räksjön (depth 4.3 m, 0 to $40\ W\ m^{-2}$; Venäläinen et al., 1999), in Finnish Lake Valkea-Kotinen (depth 2.5 m; −45 to $32\ W\ m^{-2}$; Nordbo et al., 2011) and in Ross Barnett Reservoir, in the USA (depth 5 m; 0 to $45\ W\ m^{-2}$; Liu et al., 2009).

The latent heat flux λE also showed small diurnal variations. At DPK, the strongest λE occurred at 13:30 with a composite mean value of $80.6\ W\ m^{-2}$ and the minimum of $60.1\ W\ m^{-2}$ at 6:00. Unlike land ecosystems, nocturnal evaporation was quite high, averaged at $65.5\ W\ m^{-2}$ for the hours from 18:30 to 6:00, emphasizing the importance of the nighttime measurement in the assessment of the hydrological and energy budget of the lake. Nighttime evaporation loss was maintained by the energy stored in the water volume during the daytime. On the annual basis, nighttime evaporation accounted for 48% of the total evaporation at Lake Taihu, which is similar to the value reported for a temperate reservoir in 2008 (Liu et al., 2012a).

4.4. Spatial variations in the evaporation and energy fluxes across the lake

Spatial variations in the evaporation and energy fluxes were evaluated at multiple temporal scales (diurnal, seasonal and

Table 2
Annual mean meteorological variables, radiation components and energy fluxes from September 2011 to August 2012.

Site	T_a (°C)	U ($m\ s^{-1}$)	RH (%)	T_{w20}/T_{s5} (°C)	$K_\downarrow$ ($W\ m^{-2}$)	$K_\uparrow$ ($W\ m^{-2}$)	$L_\downarrow$ ($W\ m^{-2}$)	$L_\uparrow$ ($W\ m^{-2}$)	α	R_n ($W\ m^{-2}$)	H ($W\ m^{-2}$)	λE ($W\ m^{-2}$)	β
DS	17.0	2.3	67.3	19.2	144.6	27.3	361.5	411.3	0.19	67.6	24.8	43.1	0.58
MLW	16.6	2.4	67.9	17.8	145.3	9.0	362.2	406.7	0.06	91.8	10.7	80.1	0.13
DPK	16.6	3.7	70.7	17.4	142.9	11.2	367.7	407.3	0.08	92.0	9.8	80.8	0.12

T_a, air temperature; U, wind speed; RH, relative humidity; T_{w20}, water temperature at 20 cm depth at MLW and DPK; T_{s5}, soil temperature at 5 cm depth at DS; $K_\downarrow$, incoming shortwave radiation; $K_\uparrow$, reflected shortwave radiation; $L_\downarrow$, incoming longwave radiation; $L_\uparrow$, outgoing longwave radiation; α, surface albedo; R_n, net radiation; H, sensible heat flux; λE, latent heat flux; β, Bowen ratio.

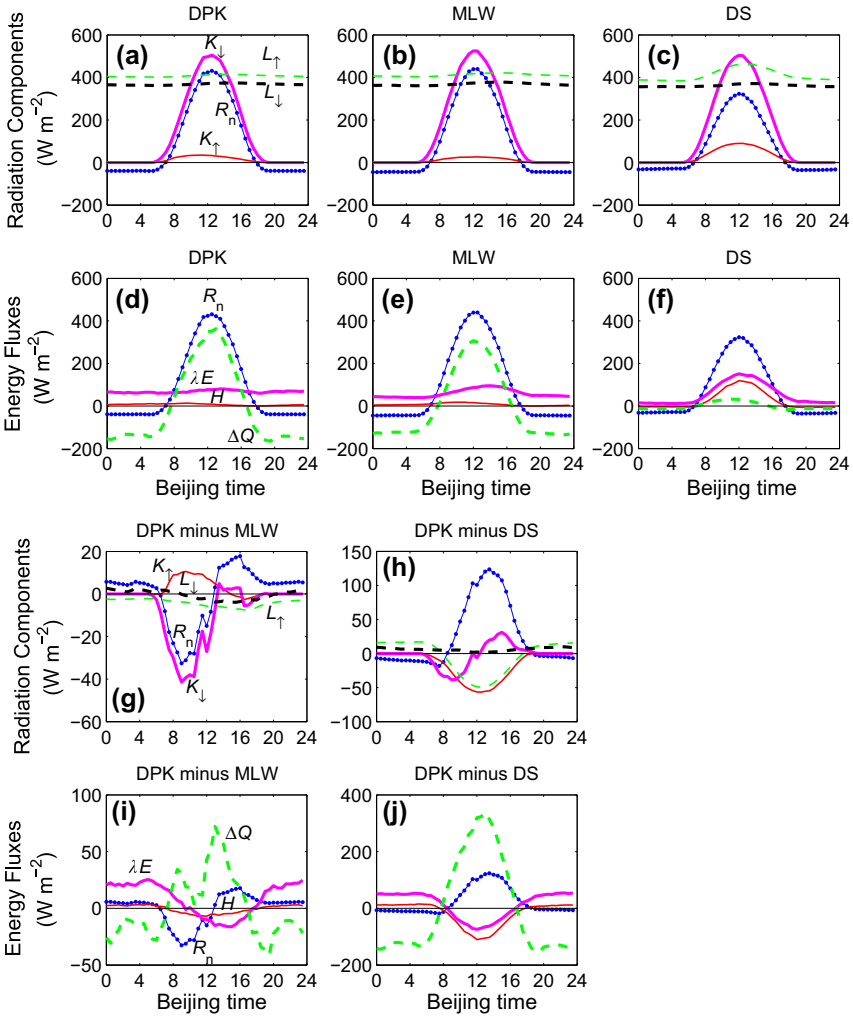

Fig. 4. Diurnal composite of radiation and energy balance components from September 2011 to August 2012 at DPK, MLW and DS sites.

annual) among the three measurement sites on Lake Taihu. The three sites had nearly identical air temperature T_a but different wind speed U (Fig. 3a, Table 2). According to the modeling study by Deng et al. (2013), the lake surface temperature is insensitive to wind speed, increasing by 0.3 °C for a 50% decrease in wind speed. The nearly identical surface temperature among the three sites (Fig. 3b) corroborated their modeling result.

The contrast in the radiation components between DPK and MLW is shown in Fig. 4g as the difference in the diurnal composites (The BFG site does not have a full annual dataset for a similar comparison.). The largest difference was found of the incoming shortwave radiation $K_{\downarrow}$ at 9:00; at this time, this component was 41.1 W m^{-2} higher at MLW site than at DPK site. We interpret this as an indication of slightly higher cloudiness at DPK in the morning. The higher cloudiness contributed at least partly to the higher albedo (Katsaros et al., 1985) at DPK (annual mean 0.08) than at MLW (annual mean 0.06; Table 2).

Turning attention now to the energy balance components, the largest contrast occurred in heat storage ΔQ (Fig. 4i) due to the difference in water depth between these two sites. The ΔQ difference (DPK minus MLW) was 72.2 W m^{-2} at 13:00 and was −41 W m^{-2} at around 19:30. As a result, the evaporation flux (as measured here by λE) showed clear spatial variations at the diurnal time scale. Due to the extra heat release from the water at night, the nighttime (18:30–6:00) λE at DPK was 20.4 W m^{-2} higher than at MLW. In the mid-afternoon, the extra heat storage at DPK caused the λE to be 16.2 W m^{-2} lower than at MLW. The difference in H was small (<7.3 W m^{-2}) between DPK and MLW.

At the monthly to the seasonal time scale, the energy fluxes were nearly identical among the three lake sites (Fig. 3d–g; Table 2). At these longer time scales, evaporative flux is insensitive to water depth. The water at MLW and DPK was more polluted than at BFG (Wang et al., 2011). Another difference is that submerged macrophytes were abundant at BFG but were absent at MLW and DPK. The lack of spatial variations indicate a lack of sensitivity of the turbulent fluxes to water quality and the influence of the submerged vegetation at least on the monthly time scale, even though water quality can interfere with solar radiation penetration in the water (Deng et al., 2013) and the presence of submerged vegetation can reduce the momentum roughness (Xiao et al., 2013). In comparison, Lofgren and Zhu (2000), Spence et al. (2011) described some spatial variations in turbulent fluxes across Lake Huron and Lake Superior. The lack of spatial variations implies that at this shallow lake, evaporation was strongly controlled by the available radiation energy and was insensitive to the biophysical properties of the water itself.

The results in Fig. 3 and Table 2 suggest that the land influence on the monthly and annual mean turbulent fluxes was small at MLW despite its close proximity to the shoreline (distance 150 m). To support this inference, we computed the flux footprint using the model proposed by Hsieh et al. (2000). Using a momentum roughness from Deng et al. (2013), the peak contribution of

the surface source to the observed flux occurred a distance of 88 m and 27 m away from the EC instrument under neutral stability ($z/L = 0$, where z is the measurement height and L is the Obukhov length) and unstable conditions ($z/L = -0.1$), respectively. Under stable conditions ($z/L = 0.1$), the peak distance extended to 207 m. Fortunately, stable stability (that is, negative H) occurred less than 7% of the observations.

4.5. Annual mean fluxes

On the annual basis (from September 2011 to August 2012), the difference in the radiation components between MLW and DPK was within the measurement uncertainty (5 W m^{-2}) of the radiometer (Table 2). Owing to more turbid water and cloudier weather at DPK, the annual mean albedo was 0.02 higher than at MLW. Averaged over the annual scale, the heat storage ΔQ was zero, indicating that the lake was neither a heat sink nor a heat source. The difference in H and λE was less than 1 W m^{-2} between the two sites with nearly identical annual Bowen ratio of 0.12–0.13.

The observed annual mean albedo is in good agreement of the values used in climate models for water bodies which vary between 0.06 and 0.08 (Cogley, 1979; Henderson-Sellers, 1986; Henderson-Sellers and Wilson, 1983; Parker et al., 1970). Shallow lakes are typically more turbid than deep ones owing to wind-induced suspension of sediment particles (Jackson, 2003). Stefan et al. (1982) showed that the presence of suspended sediment should increase water surface albedo by an amount that depends on sediment load. That our observed values did not differ much from those of clear water implies that this effect was minor at Lake Taihu.

On the basis of the Priestley–Taylor relationship (Priestley and Taylor, 1972), Brutsaert (1982) expresses the Bowen ratio β over a water body as a function of the slope of the saturation vapor pressure curve. His expression suggests that β should have a negative relationship with air temperature. The tropical Lake Tanganyika had a small annual Bowen ratio of 0.06 (Verburg and Antenucci, 2010). Yin and Nicholson (1998) estimated an annual β of 0.15 for Lake Victoria in tropical Africa. For the subtropical Lake Ikeda and Ross Barnett Reservoir, the annual β was 0.19 (Momii and Ito, 2008) and 0.20 (Liu et al., 2012a), respectively. In North America, Mirror Lake (Rosenberry et al., 2007), Sparkling Lake (Lenters et al., 2005) and Lake Williams (Rosenberry et al., 2007) had a mean β of 0.27, 0.23 and 0.25, respectively during the open-water period. A multi-year EC observation yielded a slightly higher value of 0.38 for Lake Superior (Blanken et al., 2011). Further north in the boreal Canada, much higher β values have been reported for the Great Slave Lake (0.61) and for the Great Bear Lake (0.82) during open-water seasons (Rouse et al., 2008). Our β value (0.12–0.13) is lower than most of the published annual values owing to a high annual mean lake temperature. According to the Priestley–Taylor model (Priestley and Taylor, 1972), β should decrease with increasing temperature.

The annual evaporation rate determined with the EC method does not agree with a previous estimate based on the lake water balance. The cumulative evaporation was 1061 mm and 1109 mm at MLW and DPK respectively in the 12 month period from September, 2011 to August, 2012 (Fig. 5), and was slightly less than the total precipitation measured during the same period at the surface weather stations in Wuxi (1124 mm), Dongshan (1131 mm) and Huzhou (1405 mm) (Fig. 1). According to a water balance study based on a survey of 115 rivers connected to Lake Taihu, the annual lake evaporation is only 760 mm for the period from May 2001 to April 2002 (Qin et al., 2007). The most likely reason for this discrepancy lies in the difficulty of deriving evaporation as a small residual of two large terms of the water balance: the lake inflow and outflow. According to Qin et al. (2007), these two terms are five times as large as the evaporative loss. That the combination lake evaporation models yielded similar annual evaporation estimates to the EC value (supplementary Table 2) further supports the interpretation that the water balance estimate was biased low.

4.6. Comparison between the lake and the land sites

In this section, we compare the radiation and energy balance components at DPK, a lake site with open fetch, with those measured on land at DS (Fig. 1), at the diurnal, monthly and annual scales. Obvious diurnal contrast existed in the two shortwave radiation components $K_{\downarrow}$ and $K_{\uparrow}$ and the outgoing longwave radiation $L_{\uparrow}$ (Fig. 4h). The incoming shortwave radiation $K_{\downarrow}$ was lower in the morning and higher in the afternoon at DPK than at DS. This spatial variation may have been related to local cloud cover associated with lake–land thermal circulations. The daytime reflected shortwave radiation $K_{\uparrow}$ and the outgoing longwave radiation $L_{\uparrow}$ were lower at DPK, due to smaller albedo and cooler surface temperature than at DS, with the largest differences of 56.6 and 49.4 W m^{-2} occurring at 12:30, respectively. As a result, the lake water at DPK received much higher R_n than the land at DS in the daytime, with the peak difference of 123.7 W m^{-2} observed at 13:30. At night, $L_{\uparrow}$ and $L_{\downarrow}$ were 14.9 W m^{-2}, 8.1 W m^{-2} higher at

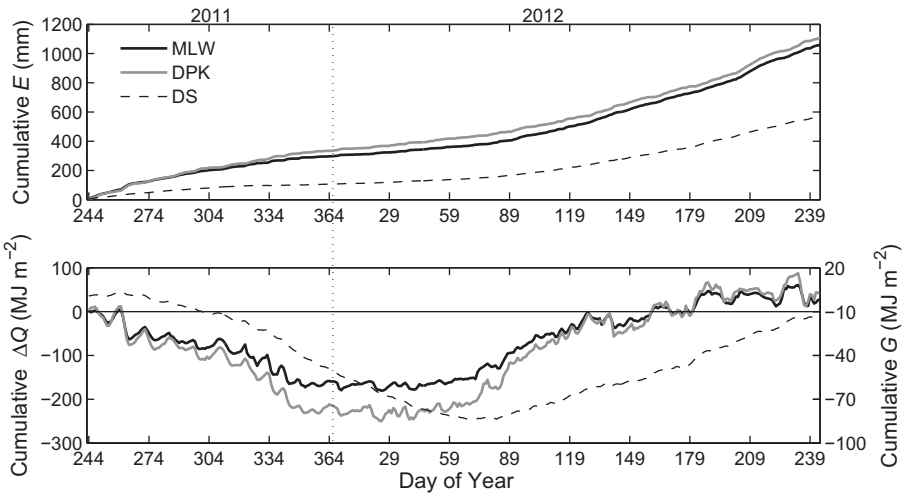

Fig. 5. Cumulative evaporation (E; top panel) and heat storage in water (ΔQ; bottom panel) or soil (G; bottom panel) for two lake sites (MLW and DPK) and one land site (DS) from September 1 2011 to August 31 2012.

DPK than at DS, respectively, resulting in 6.8 W m^{-2} lower R_n received at DPK.

With regard to the energy balance components, the two turbulent fluxes (H and λE) showed little diurnal variations at DPK as noted above but large variations at DS (Fig. 4d and f). The largest difference was detected in the heat storage due to the much greater effective heat capacity of water than that of soil. In addition, eddy motions in water enable heat to diffuse deeper than in soil by molecular heat conduction (Vallis, 2011). The heat storage difference (DPK minus DS) was positive during the day, achieving the maximum of 337.6 W m^{-2} at 13:00, and always negative during nighttime with an average difference of −133.3 W m^{-2}. The extra heat storage at DPK caused the daytime H and λE to be lower than at DS; at 12:00, these differences were −74 and −110 W m^{-2}, respectively. In contrast, the nighttime extra heat release from the lake fueled 11.1 W m^{-2} and 50 W m^{-2} more sensible and latent heat flux, respectively, to the atmosphere at DPK from 18:30 to 6:00.

The monthly mean energy fluxes are different between the two sites (Fig. 3). The monthly R_n was higher at DPK than at DS throughout the year, with the largest contrast of 46.5 W m^{-2} observed in May 2011 (Fig. 3f). The monthly H was lower at DPK than at DS, with the largest difference (−34.7 W m^{-2}) occurring in April 2012 (Fig. 3d). The monthly λE was higher at DPK than at DS (Fig. 3e), with the largest difference of 69.9 W m^{-2} in September 2011.

The small magnitude of the monthly heat storage at DS confirms that heat conductance in the soil was less effective than in the lake water (Fig. 3g). The lake behaved as a heat sink ($\Delta Q > 0$) from January to July and a source ($\Delta Q < 0$) from August to December, whereas the land switched from being a heat sink to a heat source in October. The cumulative sum of the heat storage also indicates a two-month phase lag between DPK and DS (Fig. 5). The more fluctuating monthly heat storage and its cumulative sum at DPK was a result of the higher sensitivity of lake energy balance to environmental factors such as cold front incursions (Blanken et al., 2000, 2003; Liu et al., 2011; Rouse et al., 2003; Schertzer et al., 2003).

The annual mean differences are summarized in Table 2. The annual mean H at DPK was less than half of that at DS. The pattern was reversed for λE. The annual mean Bowen ratio at DPK was only 0.12, or 20% of that at DS. If we use the lake λE as the reference state with unlimited water supply, soil moisture availability at the DS land site limited the land evapotranspiration by ~45%.

Our lake–land contrast is greater than that at Lake Superior (Fig. 6). The University of Michigan Biological Station (UMBS; Schmid et al., 2003), a deciduous broadleaf forest site, was selected as the adjacent land site to Lake Superior for this comparative analysis. Two-year (October 2008 to September 2010) turbulent flux data at UMBS archived by AmeriFlux (http://public.ornl.gov/ameriflux/dataproducts.shtml) were analyzed for comparison with the observations conducted at Lake Superior (Blanken et al., 2011). For the Lake Superior and UMBS site pair, the annual H was nearly identical and the lake λE exceeded that from the land by about 20 W m^{-2}. The Bowen ratio of Lake Superior was 39% lower than that at UMBS. In the present study, the Bowen ratio of Lake Taihu was 79% lower than the land value. It appears that in the Lake Taihu catchment, land evaporation was more limited by the availability of soil moisture, resulting in a larger lake–land contrast. Additionally Lake Taihu will have lower Bowen ratio than Lake Superior because the former is much warmer.

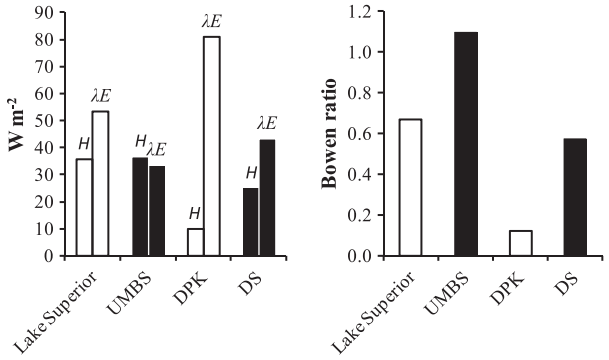

Fig. 6. Annual mean turbulent fluxes and Bowen ratio at two lake-land site pairs: Lake Superior (Blanken et al., 2011; Spence et al., 2011) versus the University of Michigan Biological Station (UMBS) (Schmid et al., 2003), and Lake Taihu (DPK) versus DS land site. Open bars denote lake observations and filled bars denote land observations.

Venäläinen et al. (1999) compared the sensible and latent heat fluxes between two Swedish lakes and an adjacent forest site. They found that during the warm season (May to September) the Bowen ratio of the Lake Råksjön and Lake Tämnaren was only 24–37% of that at the forest site.

4.7. Evaluation of evaporation models against the EC observation

The comprehensive dataset we have obtained provides an excellent opportunity for testing various lake evaporation models. In this section, monthly evaporation (in mm d^{-1}) was simulated with the 19 evaporation models (Supplementary Table 1) with inputs of meteorological and radiation data from the MLW site (26 months) and the DPK site (12 months) and then compared with the EC observations. The model skill is graphically summarized by a Taylor diagram (Fig. 7; Taylor, 2001). In the diagram, the similarity between the modeled and the observed results was quantified in terms of linear correlation coefficient, root mean square difference (RMSD) and standard deviation. Therefore, the simulated patterns that agree well with the observations should lie near the point marked "EC" (Fig. 7). Monthly differences between the simulations and the EC observations are also presented (Supplemental Fig. 1). All the models have captured the seasonal variation in the lake evaporation, showing high correlation (>0.8) with the EC observations (Fig. 7). A rigorous validation should go beyond the seasonal variations to look at residues after the seasonal signal has been removed (Lofgren et al., 2011).

Among the five groups of models, the combination group agreed most closely with the EC observations, emphasizing the importance of energy balance observation for lake evaporation prediction. The Bowen ratio energy budget method, which is widely considered as the standard when EC is unavailable (Elsawwaf et al., 2010b; Rosenberry et al., 2007; Winter et al., 1995), had the highest accuracy at both the monthly and the annual scale (Fig. 7; Supplementary Table 2 and Fig. 1). The Penman method and the Brutsaert–Stricker method had systematical biases at the monthly and annual scales (Supplementary Table 2 and Fig. 1). The Penman method overestimated the annual (September, 2011–August, 2012) evaporation by 13%, while 17% underestimate was found in the Brutsaert–Stricker method at the MLW site. Moreover, the error of the two methods was sensitive to wind speed, having a larger bias for the windier DPK site (Supplementary Table 2). Intercomparison within the combination group supports the finding that the most influential model input is ΔQ followed by the radiation parameter (Elsawwaf et al., 2010a; Rosenberry et al., 2007).

The Priestley–Taylor model with the standard coefficient value of 1.26 is often used to estimate lake evaporation in the absence of direct flux measurement (Priestley and Taylor, 1972; Stewart and Rouse, 1976). The monthly mean coefficient at the MLW site varied from 1.14 in 2010 July to 1.94 in 2011 January. The annual mean

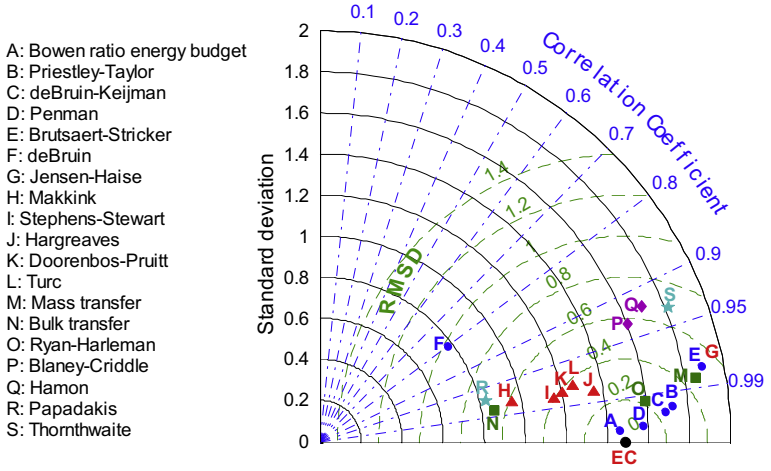

Fig. 7. A Taylor diagram showing the relative performance in the 19 evaporation models (Online Supplement) compared to the eddy covariance observations (marked as EC) at the MLW site from July, 2010 to August, 2012. The RMSDs and standard deviations are indicated by green and black arcs, respectively. The blue contours indicate the correlation coefficients. The 19 evaporation models were assigned by letters and classified into five groups (blue dots: the combination group; red triangles: the solar radiation–temperature group; green squares: the Dalton group; purple prismatic: the temperature–daylength group; cyan stars: the temperature group). (For interpretation of the references to color in this figure legend, the reader is referred to the web version of this article.)

value (from September, 2011 to August, 2012) was 1.34 and was in the middle of the range (1.15–1.45) reported in the literature (Debruin and Keijman, 1979; Hobbins et al., 2001; McAneney and Itier, 1996). Our observed Priestley–Taylor coefficient is about 0.08 greater than the standard value, indicating a moderate advection (Venäläinen et al., 1998) occurring at this near-shoreline site. At the more offshore DPK site with open fetch, the annual coefficient (1.29) was much closer to the standard value. The positive bias in the MLW Priestley–Taylor coefficient would result in 50 mm, or 4% overestimation of the annual lake evaporation. In other words, the annual lake evaporation was insensitive to the near-shore advective influence.

The six radiation–temperature based models compared less favorably (RMSD 0.3–0.6 mm d^{-1}) with most of the combination methods (RMSD 0.1–0.5 mm d^{-1} except the deBruin model; Fig. 7). Among this group, the Hargreaves model showed the best performance, while the Makkink and the Stephens–Stewart model yielded substantial negative biases (Supplementary Fig. 1). The Jensen–Haise and the Doorenbos–Pruitt model biased seasonally with opposite extents (Supplementary Fig. 1) which would cancel out when integrated over the annual cycle resulting in good agreement with the EC observations (Supplementary Table 2). The results indicate that the performance of these empirical models is climate-dependent. The Hargreaves model (Hargreaves, 1975) turned out to be the most precise one because it was developed for a warm and humid climate similar to that at Lake Taihu, while the Jensen–Haise model, developed for the arid western U.S. (Jensen and Haise, 1963) and the Makkink model, developed for the cold Netherland (Makkink, 1957; McGuinness and Bordne, 1972), presented the poorest estimates.

The three Dalton models had variable accuracy. The mass transfer and bulk transfer models ranked badly, while the Ryan–Harleman model ranked much better (Fig. 7). The transfer coefficient parameterized as a function of the lake surface area (Harbeck, 1962) or obtained from marine observations (Garratt, 1992) is not appropriate for Lake Taihu (Xiao et al., 2013).

The models containing temperature and daylight length showed unsatisfactory results (Fig. 7; Supplementary Table 2 and Fig. 1). The Blaney–Criddle model, originally designed for the western U.S. (McMahon et al., 2013), systematically overestimated the monthly evaporation (Supplementary Fig. 1), resulting in a large annual bias of 55% at the two sites (Supplementary Table 2). The two temperature-based models underestimated the lake evaporation by 28% (the Papadakis model) and 20% (the Thornthwaite model) (Supplementary Table 2).

5. Conclusions

This study aims to investigate the temporal and spatial variations in evaporation and energy balance across Lake Taihu and to evaluate the accuracy of conventional evaporation models with the EC observations. The key findings are:

(1) At the diurnal time scale, heat storage had a similar behavior to net radiation with comparable magnitudes. Nocturnal evaporation, fueled by heat release from the water column, was a major component of the local hydrologic cycle, contributing to 48% of the annual evaporation. Owing to the high temperature, its annual Bowen ratio was very small (0.12–0.13). A previous estimate of the lake annual evaporation, based on water balance of the lake (Qin et al., 2007), had a large low bias of about 30% in comparison to the EC observations.

(2) The net all-way radiation was surprisingly uniform across the lake. Contrary to the hypothesis stated in the introduction, at the monthly and annual time scales, the latent heat flux also showed little spatial variations (within 16 W m^{-2} at the monthly time scale and 1 W m^{-2} at the annual scale). The lack of spatial variations implies that at this shallow lake, evaporation was dominantly controlled by the available radiation energy and was insensitive to other biophysical drivers (wind speed, water depth, water pollution status and the presence of submerged macrophytes). A practical implication is that evaporation measured at a single point can be used for the whole lake. From the modeling perspective, Lake Taihu can be parameterized as one grid cell in climate models at least on the monthly and annual scale.

(3) On the annual cycle, the land–lake thermal contrasts were larger at Lake Taihu than at Lake Superior in the temperate latitudes. The Lake Taihu latent heat flux was 37.7 W m^{-2} or 87% greater than that of an adjacent land site. Its sensible

heat flux was 15 W m^{-2} or 60% less than that at the land site. More comparative studies are needed to confirm if the results obtained for these two lake catchments are typical of subtropical and temperate lakes.

(4) Among the 19 widely used evaporation models, the combination models, which are constrained by energy balance principles and uses the observed net radiation as an input parameter, ranked the best in the lake evaporation estimates at the monthly and annual scale. For example, the Priestley–Taylor model agreed well with the observed annual evaporation with an annual bias of less than 4%. These results provide further support for our conclusion that it was the available radiation energy that exerted dominant control on evaporation of this lake.

Acknowledgements

This study was supported by the Ministry of Education of China (Grant PCSIRT), the Priority Academic Program Development of Jiangshu Higher Education Institutions (PARD), the National Program on Key Basic Research Project of China (Grant 2010CB428502), the National Natural Science Foundation of China (Grant 41275024 and 31100359) and the Natural Science Foundation of Jiangsu Province (Grant BK2011830). The first author also acknowledges the support from the Jiangsu Innovation Program for Graduate Education (Grant N0782002075) and a visiting scholarship from China Scholarship Council.

Appendix A. Supplementary material

Supplementary data associated with this article can be found, in the online version, at http://dx.doi.org/10.1016/j.jhydrol.2014.02.012.

References

Arya, S.P., 2001. Introduction to Micrometeorology, second ed. Academic Press, New York, pp. 29–32.

Assouline, S., Mahrer, Y., 1996. Spatial and temporal variability in microclimate and evaporation over Lake Kinneret: experimental evaluation. J. Appl. Meteorol. 35, 1076–1084.

Aubinet, M., Grelle, A., Ibrom, A., Rannik, U., Moncrieff, J., Foken, T., Kowalski, A.S., Martin, P., Berbigier, P., Bernhofer, Ch., Clement, R., Elbers, J., Granier, A., Grunwald, T., Morgenstern, K., Pilegaard, K., Rebmann, C., Snijders, W., Valentini, R., Vesala, T., 2000. Estimates of the annual net carbon and water exchange of forests: the EUROFLUX methodology. Adv. Ecol. Res. 30, 113–175.

Bai, X., Wang, J., 2012. Atmospheric teleconnection patterns associated with severe and mild ice cover on the Great Lakes, 1963–2011. Water Qual. Res. J. Can. 47 (3–4), 421–435.

Baldocchi, D., Falge, E., Gu, L., Olson, R., Hollinger, D., Running, S., Anthoni, P., Bernhofer, Ch., Davis, K., Evans, R., Fuentes, J., Goldstein, A., Katul, G., Law, B., Lee, X., Malhi, Y., Meyers, T., Munger, W., Oechel, W., Paw, U.K.T., Pilegaard, K., Schmid, H.P., Valentini, R., Verma, S., Vesala, T., Wilson, K., Wofsy, S., 2001. FLUXNET: a new tool to study the temporal and spatial variability of ecosystem-scale carbon dioxide, water vapor, and energy flux densities. Br. Am. Meteorol. Soc. 82 (11), 2415–2434.

Barr, A.G., King, K.M., Gillespie, T.J., denHartog, G., Neumann, H.H., 1994. A comparison of Bowen ratio and eddy correlation sensible and latent heat flux measurements above deciduous forest. Bound-Lay. Meteorol. 71 (1–2), 21–41.

Beer, C., Reichstein, M., Tomelleri, E., Ciais, P., Jung, M., Carvalhais, N., Rödenbeck, C., Arain, M.A., Baldocchi, D., Bonan, G.B., Bondeau, A., Cescatti, A., Lasslop, G., Lindroth, A., Lomas, M., Luyssaert, S., Margolis, H., Oleson, K.W., Roupsard, O., Veenendaal, E., Viovy, N., Williams, C., Woodward, F.I., Papale, D., 2010. Terrestrial gross carbon dioxide uptake: global distribution and covariation with climate. Science 329 (5993), 834–838.

Blanken, P.D., Black, T.A., Yang, P.C., Newmann, H.H., Nesic, Z., Staebler, R., denHartog, G., Novak, M.D., Lee, X., 1997. Energy balance and canopy conductance of a boreal aspen forest: partitioning overstory and understory components. J. Geophys. Res. Atmos. 102 (D24), 28915–28928.

Blanken, P.D., Rouse, W.R., Culf, A.D., Spence, C., Boudreau, L.D., Jasper, J.N., Kochtubajda, B., Schertzer, W.M., Marsh, P., Verseghy, D., 2000. Eddy covariance measurements of evaporation from Great Slave Lake, northwest territories, Canada. Water Resour. Res. 36 (4), 1069–1077.

Blanken, P.D., Rouse, W.R., Schertzer, W.M., 2003. Enhancement of evaporation from a large northern lake by the entrainment of warm, dry air. J. Hydrometeorol. 4, 680–693.

Blanken, P.D., Spence, C., Hedstrorm, N., Lenters, J.D., 2011. Evaporation from Lake Superior: 1. Physical controls and processes. J. Great Lakes Res. 37, 707–716.

Brutsaert, W., 1982. Evaporation into the Atmosphere: Theory, History, and Application. Kluwer Academic, Boston, pp. 209–230.

Campbell Scientific Inc, 2011. Model 109 Temperature Probe Instruction Manual. Logan, Utah, USA.

Claussen, M., 1991. Estimation of areally-averaged surface fluxes. Bound-Lay. Meteorol. 54, 387–410.

Cogley, J.G., 1979. The albedo of water as a function of latitude. Mon. Weather Rev. 107, 775–781.

Crosman, E.T., Horel, J.D., 2010. Sea and lake breezes: a review of numerical Studies. Bound-Lay. Meteorol. 137, 1–29.

Crosman, E.T., Horel, J.D., 2012. Idealized large-eddy simulations of sea and lake breezes: sensitivity to lake diameter, heat flux and stability. Bound-Lay. Meteorol. 144, 309–328.

Debruin, H.A.R., Keijman, J.Q., 1979. Priestley–Taylor evaporation model applied to a large, shallow lake in the Netherlands. J. Appl. Meteorol. 18, 898–903.

Deng, B., Liu, S., Xiao, W., Wang, W., Jin, J., Lee, X., 2013. Evaluation of the CLM4 lake model at a large and shallow freshwater lake. J. Hydrometeorol. 14 (2), 636–649.

Eaton, A.K., Rouse, W.R., Lafleur, P.M., Marsh, P., Blanken, P.D., 2001. Surface energy balance of the western and central Canadian subarctic: variations in the energy balance among five major terrain types. J. Climate. 14, 3692–3703.

Elo, P.A.-R., 2007. The energy balance and vertical thermal structure of two small boreal lakes in summer. Boreal Environ. Res. 12, 585–600.

Elsawwaf, M., Willems, P., Feyen, J., 2010a. A. Assessment of the sensitivity and prediction uncertainty of evaporation models applied to Nasser Lake, Egypt. J. Hydrol. 395, 10–22.

Elsawwaf, M., Willems, P., Pagno, A., Berlamont, J., 2010b. B. Evaporation estimates from Nasser Lake, Egypt, based on three floating station and Bowen ratio energybudget. Theor. Appl. Climatol. 100, 439–465.

Eugster, W., Kling, G., Jonas, T., McFadden, J.P., Wüest, A., MacIntyre, S., Chapin III, F.S., 2003. CO_2 exchange between air and water in an Arctic Alaskan and midlatitude Swiss lake: importance of convective mixing. J. Geophys. Res. Atmos. 108 (D12), 4362. http://dx.doi.org/10.1029/2002JD002653.

Fiebrich, C.A., Martinez, J.E., Brotzge, J.A., Basara, J.B., 2003. The Oklahoma mesonet's skin temperature network. J. Atmos. Oceanic Technol. 20, 1496–1504.

Flagg, D., Brook, J., Sills, D., Makar, P., Taylor, P., Harris, G., McLaren, R., King, P., 2008. Lake breezes in southern Ontario: observations, models and impacts on air quality. In: Borrego, C., Miranda, A.I. (Eds.), Air Pollution Modeling and Its Application XIX. NATO Science for Peace and Security Series C: Environmental Security. Springer, Dordrecht, pp. 679–680.

Foken, T., 2008. The energy balance closure problem: an overview. Ecol. Appl. 18 (6), 1351–1367.

Gallego-Elvira, B., Baille, A., Martín-Górriz, B., Martínez-Álvarez, V., 2010. Energy balance and evaporation loss of an agricultural reservoir in a semi-arid climate (south-eastern Spain). Hydrol. Process. 24, 758–766.

Garratt, J.R., 1992. The Atmospheric Boundry Layer. Cambridge University Press, New York, pp. 85–113.

Gianniou, S.K., Antonopoulos, V.Z., 2007. Evaporation and energy budget in Lake Vegoritis, Greece. J. Hydrol. 345, 212–223.

Gosnell, R., Fairall, C.W., Webster, P.J., 1995. The sensible heat of rainfall in the tropical ocean. J. Geophys. Res. Oceans. 100 (C9), 18437–18442.

Harbeck, G.E., 1962. A practical field technique for measuring reservoir evaporation utilizing mass-transfer theory. Geological Survey Professional Paper 272-E. U.S. Government Printing Office, Washington, DC, pp. 101–105.

Hargreaves, G.H., 1975. Moisture availability and crop production. Trans. Am. Soc. Agri. Eng. 18 (5), 980–984.

Henderson-Sellers, B., 1986. Calculating the surface energy balance for lake and reservoir modeling: a review. Rev. Geophys. 24 (3), 625–649.

Henderson-Sellers, A., Wilson, M.F., 1983. Surface albedo data for climatic modeling. Rev. Geophys. 21 (8), 1743–1778.

Hobbins, M.T., Ramírez, J.A., Brown, T.C., 2001. The complementary relationship in estimation of regional evapotranspiration: an enhanced Advection-Aridity model. Water Resour. Res. 37 (5), 1389–1403.

Hsieh, C.I., Katul, G., Chi, T., 2000. An approximate analytical model for footprint estimation of scaler fluxes in thermally stratified atmospheric flows. Adv. Water Resour. 23, 765–772.

Huang, C., Li, Y., Le, C., Sun, D., Wu, L., Wang, L., Wang, X., 2009. Seasonal characteristics of the diffuse attenuation coefficient of Meiliang Bay waters and its primary contributiors. Acta Ecol. Sin. 29 (6), 3295–3306.

Jackson, L.J., 2003. Macrophyte-dominated and turbid states of shallow lakes: evidence from Alberta Lakes. Ecosystems 6, 213–223.

Jensen, M.E., Haise, H.R., 1963. Estimating evapotranspiration from solar radiation. Proc. Amer. Soc. Civ. Engin., J. Irrig. Drain. Div. 89 (IR-4), 15–41.

Jonsson, A., Åberg, J., Lindroth, A., Jansson, M., 2008. Gas transfer rate and CO_2 flux between an unproductive lake and the atmosphere in northern Sweden. J. Geophys. Res. Biogeo. 113, G04006. http://dx.doi.org/10.1029/2008JG000688.

Katsaros, K.B., McMurdie, L.A., Lind, R.J., DeVault, J.E., 1985. Albedo of a water surface, spectral variation, effects of atmospheric transmittance, sun angle and wind speed. J. Geophys. Res. Oceans. 90 (C4), 7313–7321.

Laird, N.F., Kristovich, D.A.R., 2002. Variations of sensible and latent heat fluxes from a Great Lakes buoy and associated synoptic weather patterns. J. Hydrometeorol. 3, 3–12.
Lee, X., Massman, W., 2011. A perspective on thirty years of theWebb, Pearman and Leuning density corrections. Bound-Lay. Meteorol. 139, 37–59.
Lee, X., Finnigan, J., Paw, U.K.T., 2004. Coordinate systems and flux bias error. In: Lee, X., Massman, W., Law, B. (Eds.), Handbook of Micrometeorology: A Guide for Surface Flux Measurement and Analysis. Kluwer Academic Publishers, New York, pp. 33–66.
Lenters, J.D., Kratz, T.K., Bowser, C.J., 2005. Effects of climate variability on lake evaporation: results from a long-term energy budget study of Sparkling Lake, northern Wisconsin (USA). J. Hydrol. 308, 168–195.
Leuning, R., Van Gorsel, E., Massman, W.J., Isaac, P.R., 2012. Reflections on the surface energy imbalance problem. Agr. Forest Meteorol. 156, 65–74.
Liu, W.T., Katsaros, K.B., Businger, J.A., 1979. Bulk parameterization of air-sea exchanges of heat and water vapor including the molecular constrains at the interface. J. Atmos. Sci. 36, 1722–1735.
Liu, H., Zhang, Y., Liu, S., Jiang, H., Sheng, L., Williams, Q.L., 2009. Eddy covariance measurements of surface energy budget and evaporation in a cool season over southern open water in Mississippi. J. Geophys. Res. Atmos. 114, D04110. http://dx.doi.org/10.1029/2008JD010891.
Liu, H., Blanken, P.D., Weidinger, T., Nordbo, A., Vesala, T., 2011. Variability in cold front activities modulating cool-season evaporation from a southern inland water in the USA. Environ. Res. Lett. 6, 024022. http://dx.doi.org/10.1088/1748-9326/6/2/024022.
Liu, H.P., Zhang, Q., Dowler, G., 2012a. Environmental controls on the surface energy budget over a large southern inland water in the United States: an analysis of one-year eddy covariance flux data. J Hydrometeorol. 13 (6), 1893–1910.
Liu, H.Z., Feng, J., Sun, J., 2012b. Measurements of water vapor and carbon dioxide fluxes over Erhai Lake using eddy covariance technique. EGU General, Assembly, vol. 14, EGU2012-3955.
Liu, X., Zhang, Y., Yin, Y., Wang, M., Qin, B., 2013. Wind and submerged aquatic vegetation influence bio-optical properties in large shallow Lake Taihu, China. J. Geophys. Res. Biogeosci. 118 (2), 713–727.
Lofgren, B.M., Zhu, Y., 2000. Surface energy fluxes on the Great Lakes based on satellite-observed surface temperatures 1992 to 1995. J. Great Lakes Res. 26 (3), 305–314.
Lofgren, B.M., Hunter, T.S., Wilbarger, J., 2011. Effects of using air temperature as a proxy for potential evapotranspiration in climate change scenarios of Great Lakes basin hydrology. J. Great Lakes Res. 37 (4), 744–752.
Madsen, J.D., Chambers, P.A., James, W.F., Koch, E.W., Westlake, D.F., 2001. The interaction between water movement, sediment dynamics and submersed macrophytes. Hydrobiologia 444, 71–84.
Makkink, G.F., 1957. Testing the Penman formula by means of lysimeters. J. Inst. Water Eng. 11, 277–288.
McAneney, K.J., Itier, B., 1996. Operational limits to the Priestley–Taylor formula. Irrig. Sci. 17, 37–43.
McGuinness, J.L., Bordne, E.F., 1972. A comparson of lysimeter-derived potential evapotranspiration with computed values. Technical Bulletin No.1452, Agricultural Research Service, US Department of Agriculture in cooperated with Ohio Agricultural Research and Development Center, Washington, DC.
McMahon, T.A., Peel, M.C., Lowe, L., Srikanthan, R., McVicar, T.R., 2013. Estimating actural, potential, reference crop and pan evaporation using standard meteorological data: a pragmatic synthesis. Hydrol. Earth Syst. Sci. 17, 1331–1363.
Momii, K., Ito, Y., 2008. Heat budget estimates for Lake Ikeda, Japan. J. Hydrol. 361, 362–370.
Nordbo, A., Launiainen, S., Mammarella, I., Leppäranta, M., Huotari, J., Ojala, A., Vesala, T., 2011. Long-term energy flux measurements and energy balance over a small boreal lake using eddy covariance technique. J. Geophys. Res. Atmos. 116, D02119. http://dx.doi.org/10.1029/2010JD014542.
Oncley, S.P., Lenschow, D.H., Campos, T.L., Davis, K.J., Mann, J., 1997. Regional-scale surface flux observations across the boreal forest during BOREAS. J. Geophys. Res.-Atmos. 102 (D24), 29147–29154.
Oswald, C.J., Rouse, W.R., 2004. Thermal characteristics and energy balance of various-size Canadian Shield lakes in the Mackenzie River basin. J. Hydrometeorol. 5, 129–144.
Parker, F.L., Krenkel, P.A., Stevens, D.B., 1970. Physical and engineering aspects of thermal pollution. CRC Crit. Rev. Environ. Control. 1 (1–4), 101–192.
Priestley, C.H.B., Taylor, R.J., 1972. On the assessment of surface heat flux and evaporation using large-scale parameters. Mon. Weather Rev. 100 (2), 81–92.
Qin, B., Hu, W., Chen, W., Ji, J., Fan, C., Chen, Y., Gao, X., Yang, L., Gao, G., Huang, W., Jiang, J., Zhang, S., Liu, Y., Zhou, Z., 2000. Studies on the hydrodynamic processes and related factors in Meiliang Bay, Northern Taihu. J Lake Sci. 12 (4), 327–334 (in Chinese).
Qin, B., Xu, P., Wu, Q., Luo, L., Zhang, Y., 2007. Environmental issues of Lake Taihu, China. Hydrobiologia 581, 3–14.
Rosenberry, D.O., Winter, T.C., Buso, D.C., Likens, G.E., 2007. Comparison of 15 evaporation methods applied to a small mountain lake in the northeastern USA. J. Hydrol. 340, 149–166.
Rouse, W.R., Oswald, C.M., Binyamin, J., Blanken, P.D., Schertzer, W.M., Spence, C., 2003. Interannual and seasonal variability of the surface energy balance and temperature of central Great Slave Lake. J. Hydrometeorol. 4, 720–730.
Rouse, W.R., Blanken, P.D., Bussières, N., Oswald, C.J., Schertzer, W.M., Spence, C., Walker, A.E., 2008. Investigation of the thermal and energy balance regimes of Great Slave and Great Bear Lakes. J. Hydrometeorol. 9, 1318–1333.
Schertzer, W.M., Rouse, W.R., Blanken, P.D., Walker, A.E., 2003. Over-lake meteorology and estimated bulk heat exchange of Great Slave Lake in 1998 and 1999. J. Hydrometeorol. 4, 649–659.
Schmid, H.P., Su, H.B., Vogel, C.S., Curtis, P.S., 2003. Ecosystem-atmosphere exchange of carbon dioxide over a mixed hardwood forest in northern lower Michigan. J. Geophys. Res. Atmos. 108 (D14), 4417. http://dx.doi.org/10.1029/2002JD003011.
Shoemaker, W.B., Sumner, D.M., Castillo, A., 2005. Estimating changes in heat energy stored within a column of wetland surface water and factors controlling theis importance in the surface energy budget. Water Resour. Res. 41, W10411. http://dx.doi.org/10.1029/2005WR004037.
Sills, D.M.L., Brook, J.R., Levy, I., Makar, P.A., Zhang, J., Taylor, P.A., 2011. Lake breezes in the southern Great Lakes region and their influence during BAQS-Met 2007. Atmos. Chem. Phys. 11, 7955–7973.
Spence, C., Blanken, P.D., Hedstrom, N., Fortin, V., Wilson, H., 2011. Evaporation from Lake Superior: 2 Spatial distribution and variability. J. Great Lakes Res. 37, 717–724.
Stefan, H.G., Dhamotharan, S., Schiebe, F.R., 1982. Temperature/sediment model for a shallow lake. J. Environ. Eng. Asc. 108 (4), 750–765.
Stephens, G.L., Li, J., Wild, M., Clayson, C.A., Loeb, N., Kato, S., Lécuyer, T., Stackhouse, P.W., Lebsock, M., Andrews, T., 2012. An update on Earth's energy balance in light of the latest global observations. Nat. Geosci. 5 (10), 691–696.
Stewart, R.B., Rouse, W.R., 1976. A simple method for determining the evaporation from shallow lakes and ponds. Water Resour. Res. 12 (4), 623–628.
Steyn, D.G., 2003. Scaling the vertical structure of sea breezes revisited. Bound-Lay. Meteorol. 107, 177–188.
Sturrock, A.M., Winter, T.C., Rosenberry, D.O., 1992. Energy budget evaporation from Williams Lake: a closed lake in north central Minnesota. Water Resour. Res. 28 (6), 1605–1617.
Subin, Z.M., Riley, W.J., Mironov, D., 2012. An improved lake model for climate simulations: model structure, evaluation, and sensitivity analyses in CESM1. J. Adv. Model. Earth. Syst. 4, M02001. http://dx.doi.org/10.1029/2011MS000072.
Tabari, H., 2010. Evaluation of reference crop evapotranspiration equations in various climate. Water Resour. Manage 2010 (24), 2311–2337.
Tanny, J., Cohen, S., Assouline, S., Lange, F., Grava, A., Berger, D., Teltch, B., Parlange, M.B., 2008. Evaporation from a small water reservoir: direct measurements and estimates. J. Hydrol. 351, 218–229.
Tanny, J., Cohen, S., Berger, D., Teltch, B., Mekhmandarov, Y., Bahar, M., Katul, G.G., Assouline, S., 2011. Evaporation from a reservoir with fluctuating water level: correcting for limited fetch. J. Hydrol. 404, 146–156.
Taylor, K.E., 2001. Summarizing multiple aspects of model performance in a single diagram. J. Geophys. Res. Atmos. 106 (D7), 7183–7192.
Twine, T.E., Kustas, W.P., Norman, J.M., Cook, D.R., Houser, P.R., Meyers, T.P., Prueger, J.H., Starks, P.J., Wesely, M.L., 2000. Correcting eddy-covariance flux underestimates over a grassland. Agric. Forest Meteorol. 103, 279–300.
Vallis, G.K., 2011. Climate and the Oceans. Princeton University Press, Princeton, pp. 105–127.
Venäläinen, A., Heikinheimo, M., Tourula, T., 1998. Latent heat flux from small sheltered lakes. Bound-Lay. Meteorol. 86, 355–377.
Venäläinen, A., Frech, M., Heikinheimo, M., Grelle, A., 1999. Comparison of latent and sensible heat fluxes over boreal lakes with concurrent fluxes over a forest: implications for regional averaging. Agric. Forest Meteorol. 98–99, 535–546.
Verburg, P., Antenucci, J.P., 2010. Persistent unstable atmospheric boundary layer enhances sensible and latent heat loss in a tropical great lake: Lake Tanganyika. J. Geophys. Res.-Atmos. 115, D11109. http://dx.doi.org/10.1029/2009JD012839.
Vesala, T., Huotari, J., Rannik, Ü., Suni, T., Smolander, S., Sogachev, A., Launiainen, S., Ojala, A., 2006. Eddy covariance measurements of carbon exchange and latent and sensible heat fluxes over a boreal lake for a full open-water period. J. Geophys. Res. Atmos. 111, D11101. http://dx.doi.org/10.1029/2005JD006365.
Wang, J., Bras, R.L., 1999. Ground heat flux estimated from surface soil temperature. J. Hydrol. 216, 214–226.
Wang, K., Dickinson, R.E., 2012. A review of global terrestrial evapotranspiration: observation, modeling, climatology, and climatic variability. Rev. Geophys. 50, RG2005. http://dx.doi.org/10.1029/2011RG000373.
Wang, M., Shi, W., Tang, J., 2011. Water property monitoring and assessment for China's inland Lake Taihu from MODIS-Aqua measurements. Remote Sens. Environ. 115, 841–854.
Webb, E.K., Pearman, G.I., Leuning, R., 1980. Correction of flux measurements for density effects due to heat and water vapor transfer. Quart. J. Roy. Meteor. Soc. 106, 85–100.
Wilson, K.B., Baldocchi, D.D., Aubinet, M., Berbigier, P., Bernhofer, C., Dolman, H., Falge, E., Field, C., Goldstein, A., Granier, A., Grelle, A., Halldor, T., Hollinger, D., Katul, G., Law, B.E., Lindroth, A., Meyers, T., Moncrieff, J., Monson, R., Oechel, W., Tenhunen, J., Valentini, R., Verma, S., Vesala, T., Wofsy, S., 2002a. Energy partitioning between latent and sensible heat flux during the warm season at FLUXNET sites. Water Resour. Res. 38 (12), 1294. http://dx.doi.org/10.1029/2001WR000989.
Wilson, K.B., Goldstein, A., Falge, E., Aubinet, M., Baldocchi, D., Berbigier, P., Bernhofer, C., Ceulemans, R., Dolman, H., Field, C., Grelle, A., Ibrom, A., Law, B.E., Kowalski, A., Meyers, T., Moncrieff, J., Monson, R., Oechel, W., Tenhunen, J., Valentini, R., Verma, S., 2002b. Energy balance closure at FLUXNET sites. Agric. Forest. Meteorol. 113 (1–4), 223–243.
Winter, T.C., Rosenberry, D.O., Sturrock, A.M., 1995. Evaluation of 11 equations for determining evaporation for a small lake in the north central United States. Water Resour. Res. 31 (4), 983–993.

Wohlfahrt, G., Haslwanter, A., Hörtnagl, L., Jasoni, R.L., Fenstermaker, L.F., Arnone III, J.A., Hammerle, A., 2009. On the consequences of the energy imbalance for calculating surface conductance to water vapour. Agric. For. Meteorol. 149 (9), 1556–1559.

Xiao, W., Liu, S., Wang, W., Yang, D., Xu, J., Cao, C., Li, H., Lee, X., 2013. Transfer coefficients of momentum, sensible heat and water vapour in the atmospheric surface layer of a large freshwater lake. Bound-Lay. Meteorol. 148 (3), 479–494.

Yin, X., Nicholson, S.E., 1998. The water balance of Lake Victoria. Hydrolog. Sci. J. 43 (5), 789–811.

Zhang, Y., Yin, Y., Liu, X., Shi, Z., Feng, L., Liu, M., Zhu, G., Gong, Z., Qin, B., 2011. Spatial-seasonal dynamics of chromophoric dissolved organic matter in Lake Taihu, a large eutrophic, shallow lake in China. Org. Geochem. 42, 510–519.